CLAS-NOTE 2006-012
Original: August 22, 2006

Comparison of Different Schemes for Analyzing the $\Lambda(1405)$ in the g11 Data Set

Kei Moriya*
Reinhard A. Schumacher
Department of Physcis, Carnegie Mellon University,
Pittsburgh, PA 15213, USA

revised Ver. 2.1

August 21, 2006

Abstract

As of April 2006, our analysis of the lineshape and cross section of the $\Lambda(1405)$ was done on the so-called "skimmed" data set. This is a subset of the entire g11a data set requiring that every event have at least one particle identified by *either* `part` or `SEB` as a kaon. Our collaborators had recently claimed that using the skimmed data set would result in a significant loss of signal, especially in the high-momentum region[1].

The purpose of this study was twofold:

1. Investigate how much data we lose by using the "skimmed" data set compared to the entire data set.
2. Investigate how many events we recover by using the kinematic fit program as compared to the conventional cuts.

Our final results show that the kinematic fit is a good and elegant way of selecting events, but up to the % level, their is no difference between using the conventional physics cuts we had applied before, nor is there any loss of events due to using the skimmed data set. The different schemes will be used in our analysis as a cross check of the cuts we make. An overview of the cuts that we have made in the g11 data set is shown extensively.

1 Initial Motives for Comparing the Different Schemes

The final goal of our study of the g11 data set is to extract the lineshape and cross section of the 3 decay channels (4 overall topologies) of the $\Lambda(1405)$. For the past year we have been making various cuts on the g11 data for this purpose.

*kmoriya@andrew.cmu.edu

At the beginning of 2006, a simple comparison was done of the number of $p, K^+, \pi^-, (\pi^0)$ events that passed through our cuts and that passed through the kinematic fit cuts. The requirement for these events is that the particles p, K^+, π^- are detected, and the undetected π^0 is to be reconstructed via missing energy and momentum.

Fig. 1 shows this initial comparison. As can easily be seen, there is a huge discrepancy between the number of events chosen by the kinematic fit schemes and our conventional cuts. The purpose of this paper is to show that by refining our cuts, we are able to see an agreement of these schemes at the % level.

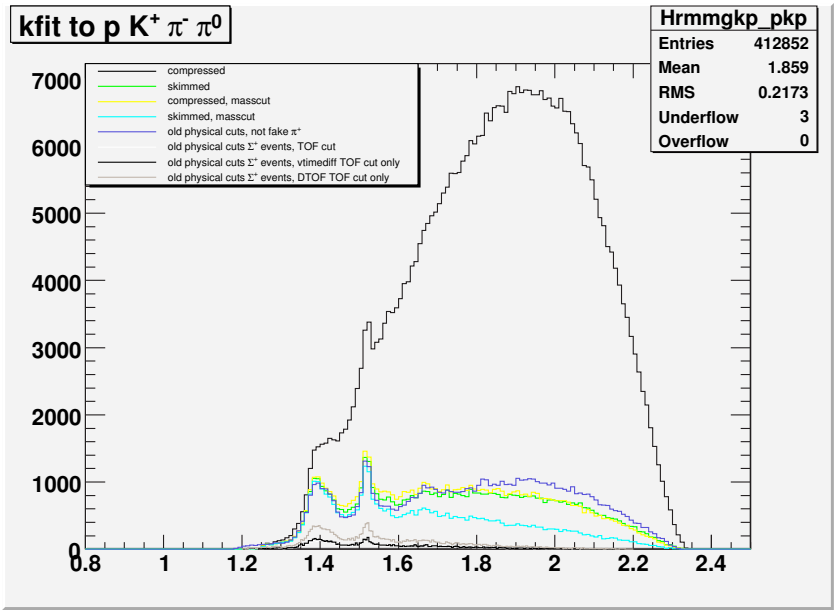

Figure 1: Comparison of MM(γ, K^+) for different schemes. A detailed explanation of each scheme will follow. At this early stage the schemes "skimmed" (green), "compressed, masscut" (yellow), and "skimmed, masscut" (light blue) fairly agree with each other, while "compressed" (top black line) has many more events, and the conventional cuts (bottom black line) has much fewer events.

In the following chapters we will describe the various cuts made on the data, the motivation for making them and their modifications. A similar description of the kinematic fit schemes will follow. All studies conducted for this paper were done solely for the topology $p, K^+, \pi^-, (\pi^0)$.

2 Conventional Physics Cuts

The conventional cuts applied for the topology $p, K^+, \pi^-, (\pi^0)$ are:

1. kaon skim
2. (absence of) $P_\perp$ cuts
3. fiducial cuts

4. fake π^+cuts

5. timing cuts

6. missing mass(MM) cuts

Below is a summary of each cut.

2.1 Kaon Skim

The entire g11 data set is compressed and stored on disc files at CMU. The entire compressed g11 data set is approximately 614 GB, and includes many events that are irrevelant to our specific studies. To optimize the speed of our analysis, a skim is needed.

The kaon skim was done by requiring that *either* of the PID schemes `part` or `SEB` identify one of the particles in the event as a kaon. For the conventional physics cuts, since `part` was used as the default PID scheme for our analysis, only events that `part` identified as having a kaon were used. This skim cuts down the size of the data set to approximately 74 GB. For the conventional physics cuts, since the events in the skim and the events in our analysis are both selected by `part` , there is no difference in using the entire compressed data set compared to the skimmed data set. We will show for the kinematic fit schemes that this skimming is an effective one indeed, and that we do not lose signal events due to this skim.

2.2 (Absence of) $P_\perp$ Cuts

After `part` identifies the charged particles p, K^+, π^-, we are able to reconstruct the missing momentum of the event. The spectrum of the polar angle of this missing momentum for each event($\theta_{\rm miss}$) is shown in Fig. 2. As can be seen in the first plot, there is a sharp rise of events at the tails of the distribution of $\cos\theta_{\rm miss}$.

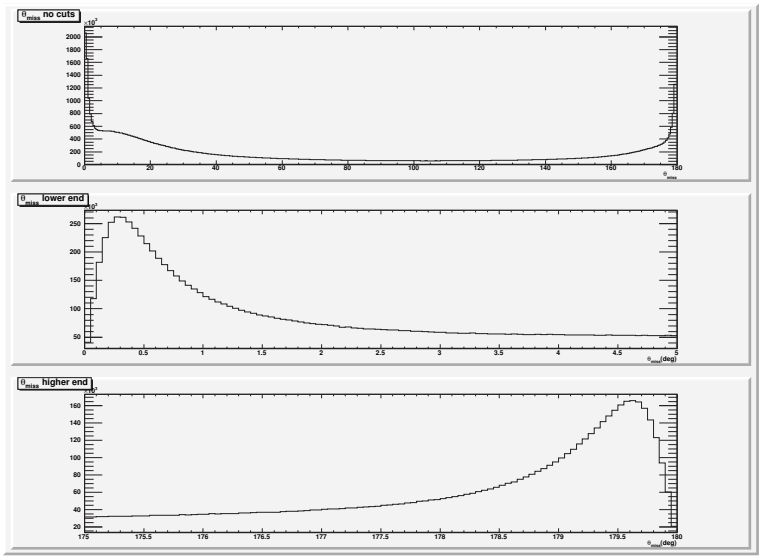

Figure 2: Polar angle of missing momentum. The top figure shows the full spectrum of the polar angle for the missing momentum. The next two show the low end and high end of the spectrum respectively.

A natural interpretation of these spikes is that the photon was misidentified, therefore leading to an excess or shortage of momentum in the polar (beam) direction. To get rid of these wrong photon events a cut was considered to be made to remove events with $0° \leq \theta_{\text{miss}} \leq 1°$ and $179° \leq \theta_{\text{miss}} \leq 180°$.

This cut rejects events with missing momentum directly in the direction of the beam line. But as can be seen from the lower two plots of Fig. 2, a close-up look at the $\cos\theta_{\text{miss}}$ distribution shows that the excess of events at the ends is not a discontinuous spike but a rather smooth bump. This is probably due to the smearing of $\cos\theta_{\text{miss}}$ since $\cos\theta_{\text{miss}}$ is rebuilt using the momenta of all three detected particles. In essence, this makes the place to make a cut quite arbitrary. A study of how such a cut would affect our studies was conducted, and it was found that the effect of including this cut is very small, and other cuts made naturally take out the events with misidentified photons (Fig. 3), since in most cases the kinematics will not collaborate to reconstruct a meaningful event in such a case. According to Fig. 3, cutting off events with $\theta_{\text{miss}} < 1°$ from the edges has less than a 0.5% effect on the missing mass spectrum and less than a 1.3% effect on the spectrum of missing mass off of the K^+ for our final selection of events (the cuts that were made will be explained below). In conclusion, the cut on $\cos\theta_{\text{miss}}$ is not well defined and furthermore does not help in increasing signal-to-noise ratio. Therefore this cut was not applied in our final selection of events.

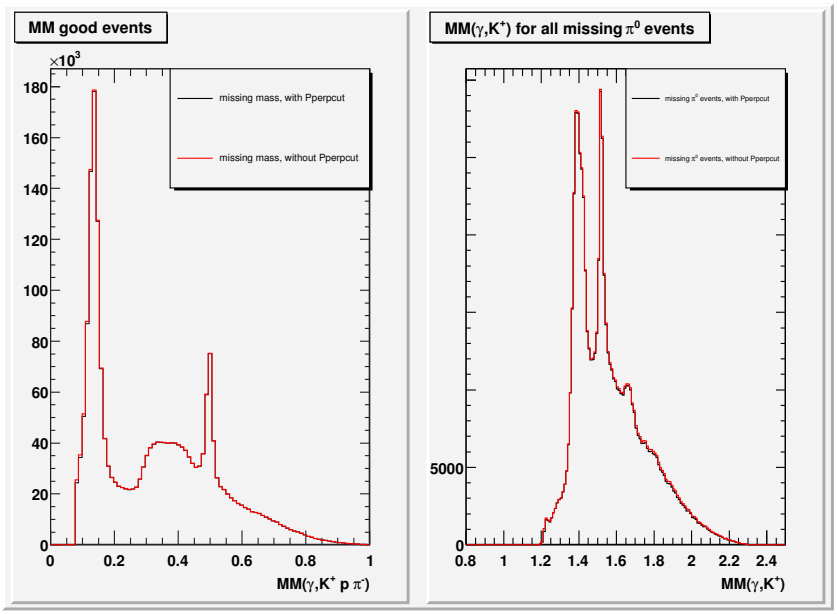

Figure 3: Effect of applying cut on $\cos\theta_{\text{miss}}$. The missing mass spectrum (left) and missing mass off of the K^+ spectrum (right) have a 0.5% and 1.3% overall difference when the cut is applied (red) compared to when the cut is not applied (black). No significant change in the shapes of the spectra can be observed.

2.3 Fiducial Cuts

The next cuts to be made were the fiducial cuts developed by Matt Bellis. This makes a curved contour cut in the forward region and a sharp cutoff that is sector dependent in the backward region. Also, only events that had hits in selected TOF paddles were chosen. The distribution of particles detected in the case of $p, K^+, \pi^-, (\pi^0)$ are shown in Fig. 4.

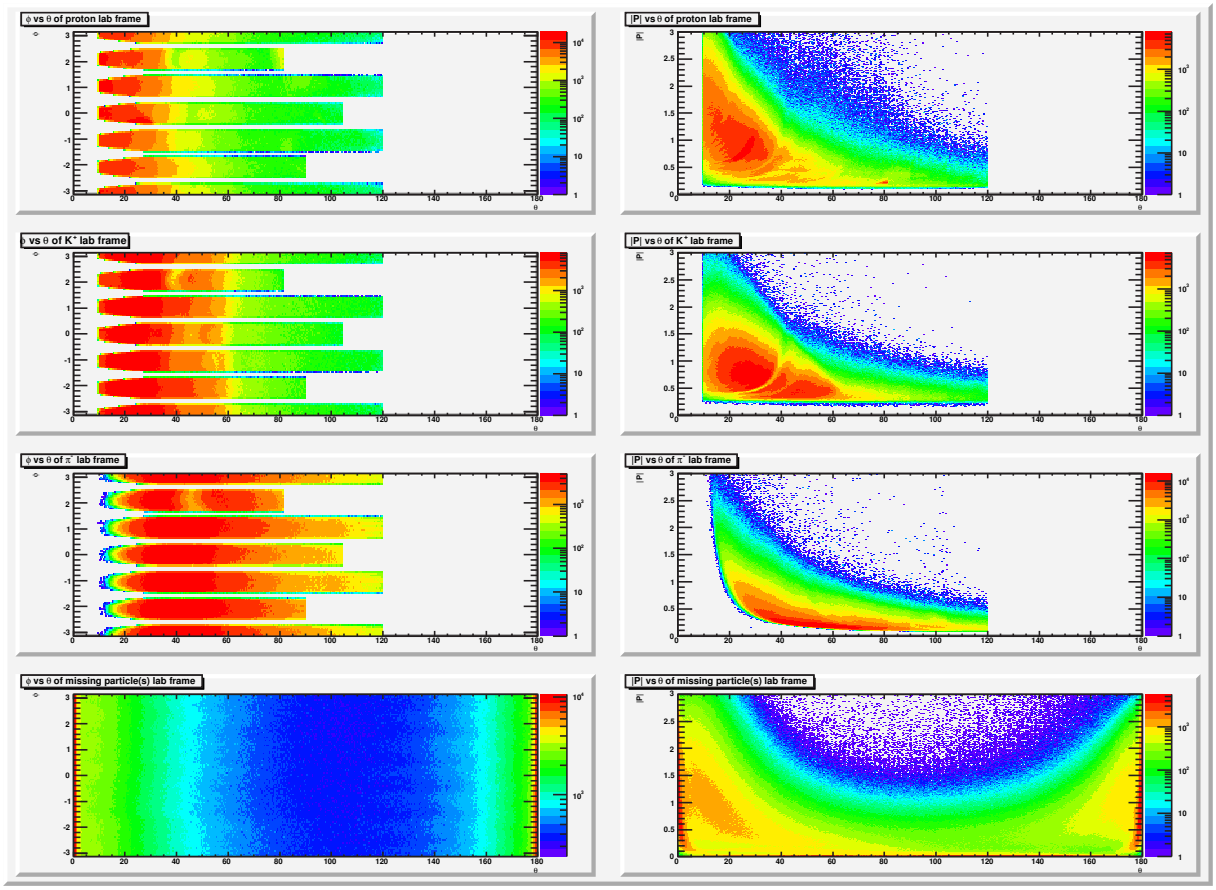

Figure 4: Angular distribution of particles after fiducial cuts. The rows correspond to p, K^+, π^-, and the missing momentum, respectively, while the columns correspond to ϕ vs θ and $|\vec{P}|$ vs θ for each particle. All plots are in the lab frame. Notice the log scale for all plots.

The fiducial cuts remove approximately 40% of the reconstructed events, but are necessary so as to make sure the particles were detected in regions of CLAS that are physically possible. The fiducial cuts are still being developed, and may be modified in the future.

2.4 Fake π^+Cuts

Whenever a kaon is required in the final state of an analysis, the main source of PID confusion is whether or not the detected particle is actually a kaon or not. To exclude events where the detected $K^+$was actually a

π^+, a missing mass squared(MM2) plot with the K^+mass changed to a π^+ mass was compared to the original MM2. This is shown in Fig. 5, and clearly shows the band of events where the $K^+$was actually a π^+.

To take out these events cuts were made to leave only the events in the upper right hand corner. This cut also rejects p, K^+, π^- exclusive events, but because we do not use these events for our analysis this was allowed.

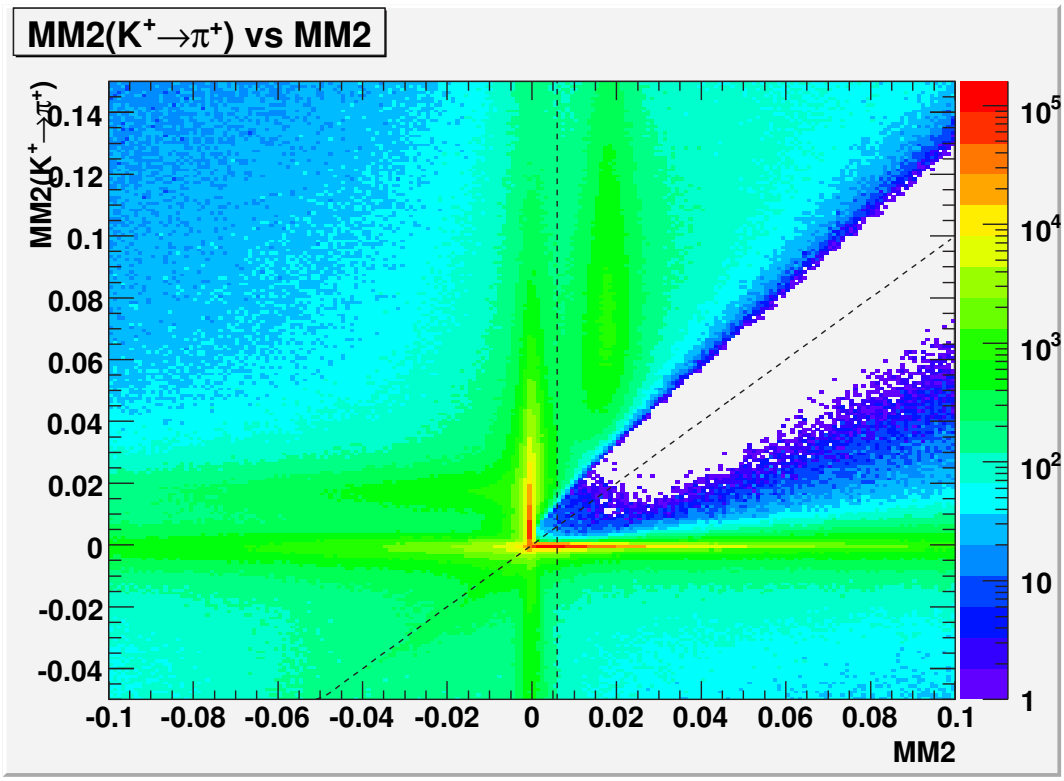

Figure 5: MM2 when the K^+mass is changed to a π^+mass against the original MM2. The horizontal bands correspond to events where the $K^+$was actually a π^+. Our events of interest are the vertical band of missing π^0events.

A similar check of changing the nominal K^+ mass to a proton mass was also done, but since there were no visible bands corresponding to K^+-proton confusion, no cut was made.

At this stage we have eliminated most events with wrong PIDs, but still have many events with the wrong timing.

2.5 Timing Cuts

Let us define the quantity ΔTOF for each detected particle as

$$\Delta\text{TOF} \equiv \text{TOF} \times \left(1 - \sqrt{\frac{M_{\text{hyp}}^2 + \vec{P}^2}{M_{\text{calc}}^2 + \vec{P}^2}} \right),$$

where TOF is the difference in timing between the incoming photon vertex time and the time that the particle hit the TOF walls, M_{hyp} is the chosen hypothetical mass of the particle, and M_{calc} is the calculated mass of the particle from its momentum and time of flight. M_{calc} is calculated as $M_{\text{calc}} = \sqrt{1-\beta^2}|\vec{P}|/\beta$ where $\beta \equiv d/\text{TOF}$ is the velocity of the particle given by the path length and time of flight of the particle. Using this relation, the above equation for ΔTOF can be simplified to

$$\Delta\text{TOF} = \text{TOF} - \frac{d}{|\vec{P}|}\sqrt{M_{\text{hyp}}^2 + \vec{P}^2}.$$

This gives a quantity that should be 0 when the particle's identity agrees with the hypothesis, positive(negative) when the actual mass of the particle is heavier(lighter) than the hypothesis mass. It turns out that this quantity when plotted against $|\vec{P}|$ is a very useful quantity to cut on, as explained below.

Before the current study, the start counter(ST) was used to determine a vertex time for each detected particle. The cut applied was $|\Delta t| =$ | (particle ST vertex time)$-$(photon vertex time)$| < 2$ ns. The problem with this cut is that the ST had only approximately a 80% chance of firing for each particle, so by requiring that the ST fired for all three detected particles, we unnecessarily lose almost half of our data. This is one of the reasons that we had much fewer events in the conventional physics cuts in Fig. 1. In an effort to recover the particles' timing information without using the ST, Matt Bellis suggested we use the TOF walls and propagate backwards to the vertex using the measured momentum of the particles. This requires a mass hypothesis for each particle, and is calculated as

$$(\text{particle vertex time}) = t_{\text{TOF}} - d/\beta,$$

where t_{TOF} is the time that the particle hit the TOF wall, d is the path length of the particle and β is calculated with the mass hypothesis M_{hyp} as $\beta = |\vec{P}|/\sqrt{M_{\text{hyp}}^2 + \vec{P}^2}$. When the difference between this quantity and the photon vertex time is taken, this just reduces to the quantity ΔTOF defined above. Therefore we see that the quantity ΔTOF is 0 only when both the particle and photon are selected for the right photon bucket(timing), and when the mass hypothesis of the particle is correct(PID).

In using ΔTOF as timing information for the particles, the question was raised whether the resolution would be comparable to that of the ST. The vertex time for each particle can be obtained by the two schemes, one using the ST and one using the ΔTOF method. In the ΔTOF scheme, for each particle detected a different vertex time will be calculated for each different assumed mass. The particles that we are using were the particles chosen by the `part` scheme.

The vertex times obtained this way are shown in Fig. 6. We see that the vertex time distribution will match the one given by the ST only if the particle is assigned a mass that coincides with the particle ID that `part` chose. Also, the distribution of the vertex time using the mass hypothesis has the same resolution as the ST as long as the hypothesis mass was chosen correctly. This is because the dominant width of the ΔTOF peaks come from the timing resolution of the TOF counters, not the pathlength or momentum measurements

and is roughly independent of $|\vec{P}|$. Therefore we do not use the ST any more, and rely solely on the ΔTOF method for timing information.

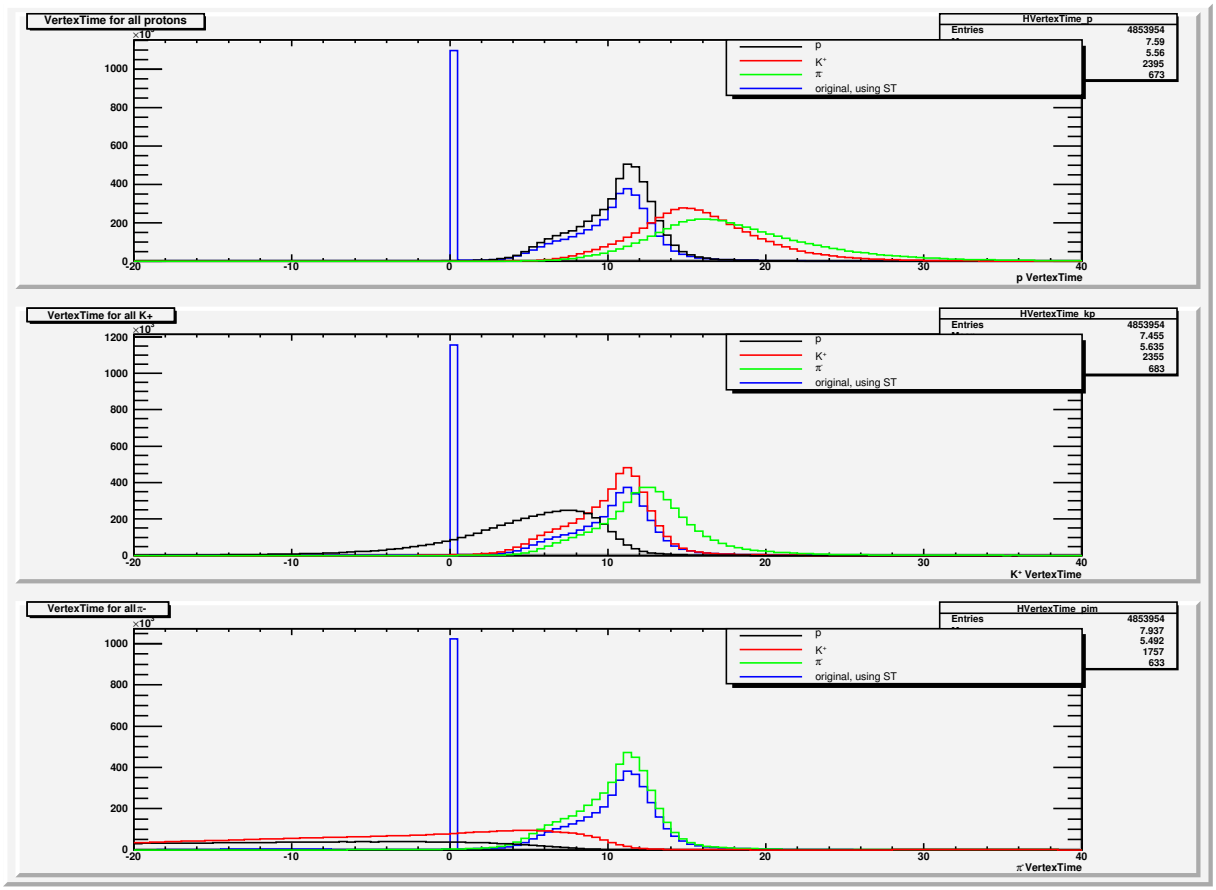

Figure 6: Comparison of the vertex time for each particle using different mass hypotheses and the ST. Notice the spike at 0 corresponding to the case when the ST did not fire. If the mass hypothesis is correct, the distribution looks the same for the ST and mass hypothesis with the same resolution. When a different mass is chosen the timing information is totally distorted compared to the ST timing.

Plotted one dimensionaly, ΔTOF has the characteristic 2 ns structure of the photon beam used in CLAS, but plotting it against $|\vec{P}|$ reveals interesting features. In Fig. 7, we see shadow bands converging to multiples of 2 ns corresponding to out of timing photons or particles. Also, for K^+ and π^-, we see bands converging from the negative side to the main band. It was found that these bands are due to lighter particles being misidentified as a kaon or a pion.

To get rid of the shadow bands, a cut was made first on the proton. The motivation behind this was because the proton has no decays, it has the cleanest distribution. A curving cut was made in the first figure of Fig. 7 as $-0.6 - 2e^{-1.5|P_p|} < \Delta\text{TOF} < 1.4 + 8e^{-5|P_p|}$, where $|P_p|$ is the magnitude of momentum of the detected proton. This cut was made so as to incorporate the main band of protons detected while cutting away the shadow bands at multiples of 2 ns. The shape of the cut was determined to take into account the

spread of the shape of the main proton band at low momenta, and made with an exponential curve to be easily modifiable. No systematic studies of the number of events against the exact shape of the cut have been made, but these effects should be negligible (Fig. 7 is plotted on a log scale).

Fig. 8 shows ΔTOF vs $|\vec{P}|$ for the 3 particles after the proton timing cut. After the proton timing cut, similar cuts were made on the $K^+$and π^-, and the end result is shown in Fig. 9. The cuts were $-0.5-4e^{-7|P_{K^+}|} < \Delta\text{TOF} < 1.4+4e^{-8|P_{K^+}|}$ for the $K^+$and $-0.4 < \Delta\text{TOF} < 1+2e^{-7|P_{\pi^-}|}$ for the π^-($|P_{K^+}|$ and $|P_{\pi^-}|$ are the magnitude of momentum of the $K^+$and π^-respectively). The cuts on the $K^+$and π^-were made asymmetric with respect to $\Delta\text{TOF} = 0$ because there was contamination in the negative ΔTOF region due to lighter particles.

This timing cut gives us a well-defined sample of events. It was found that this timing cut cuts down on background events and sharpens the physical peaks as compared to using the ST alone.

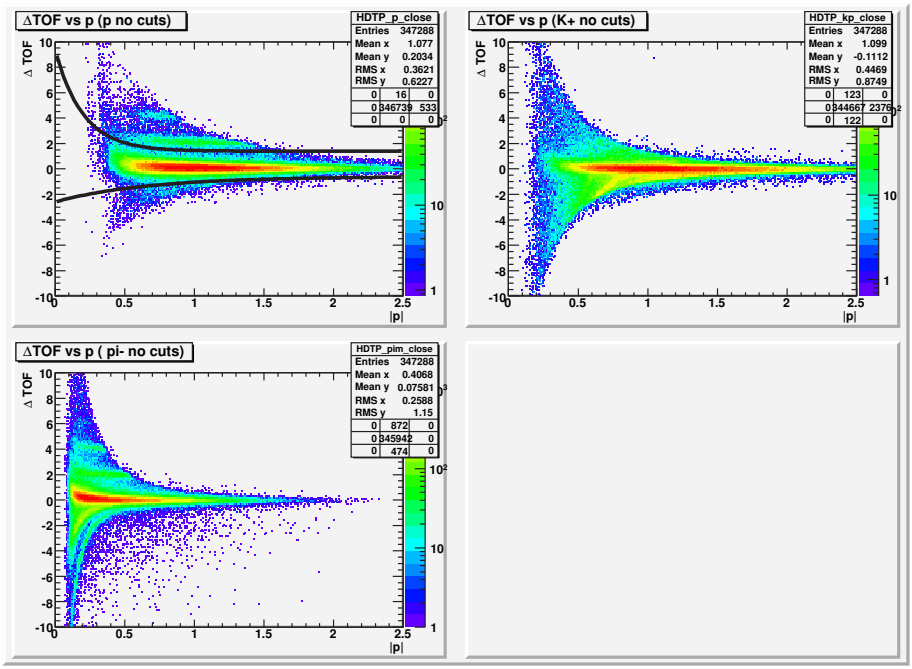

Figure 7: ΔTOF vs $|\vec{P}|$ for p, K^+, π^-. The bands converging to multiples of 2 ns correspond to shadow bands. For the $K^+$and π^-, there are bands in the negative ΔTOF region corresponding to misidentified lighter particles. For the π^-, the yellow band are muons(μ^-), and the light blue band are electrons. The black lines in the proton figure are where the cuts were made.

2.6 Missing Mass Cut

The final cut to be made is a missing mass squared(MM2) cut around the π^0mass to select a missing π^0. The MM2 distribution is shown in Fig. 10. A Gaussian with a 1st order polynomial background fit was done to

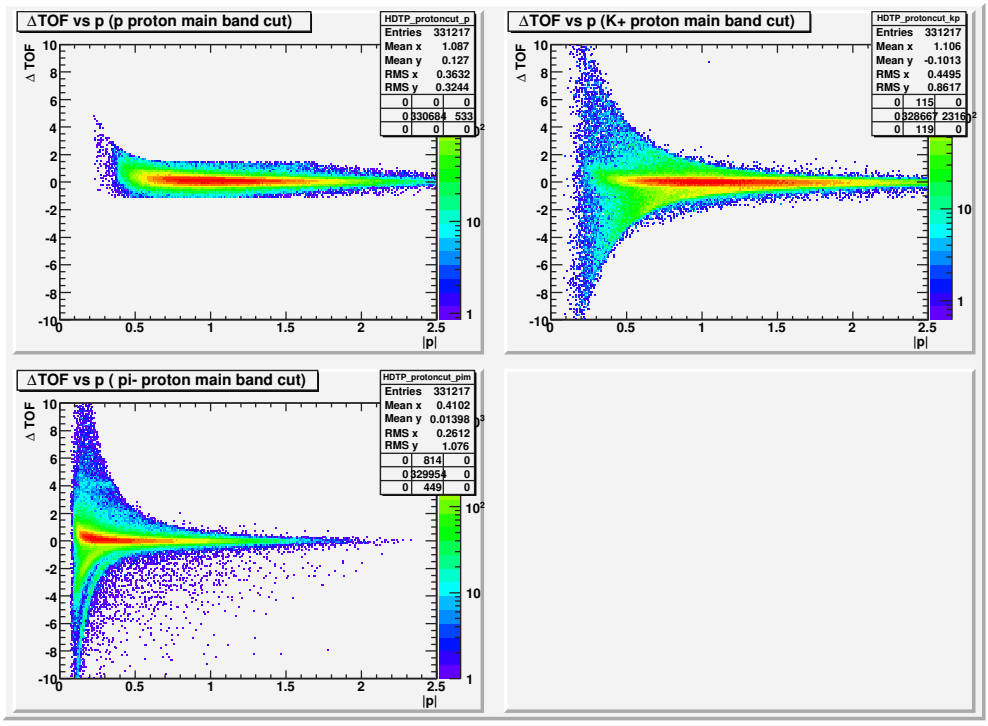

Figure 8: ΔTOF vs $|\vec{P}|$ for p, K^+, π^-after a cut was made on the proton ΔTOF.

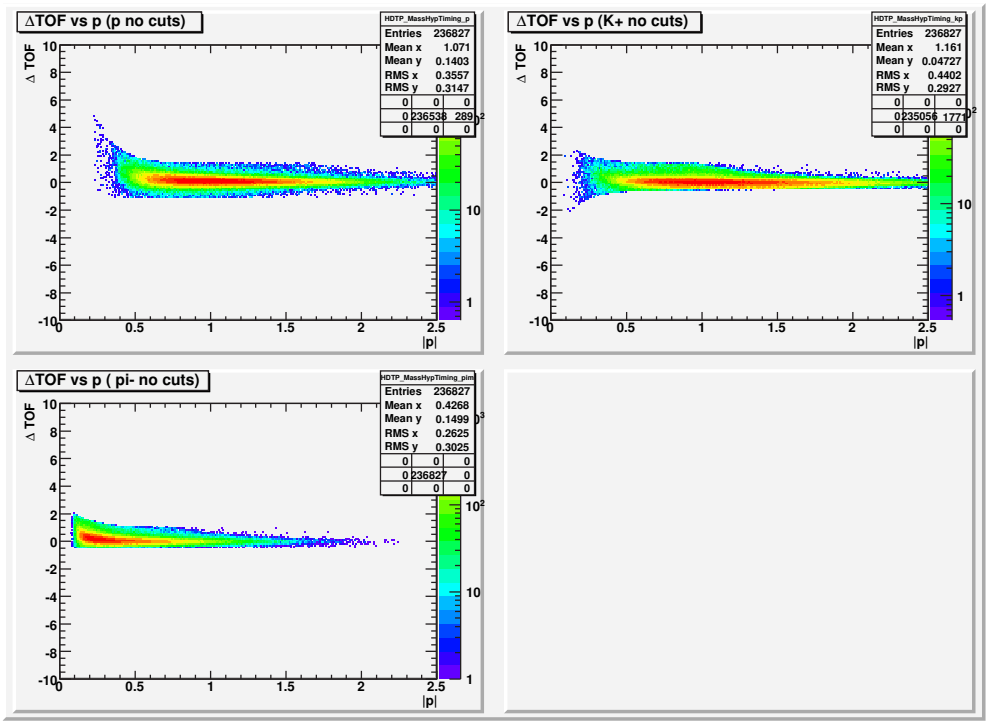

Figure 9: ΔTOF vs $|\vec{P}|$ for p, K^+, π^-after a cut was made on all particles' ΔTOF.

the π^0 peak, and an area of $\pm 3\sigma$ was chosen for the cut.

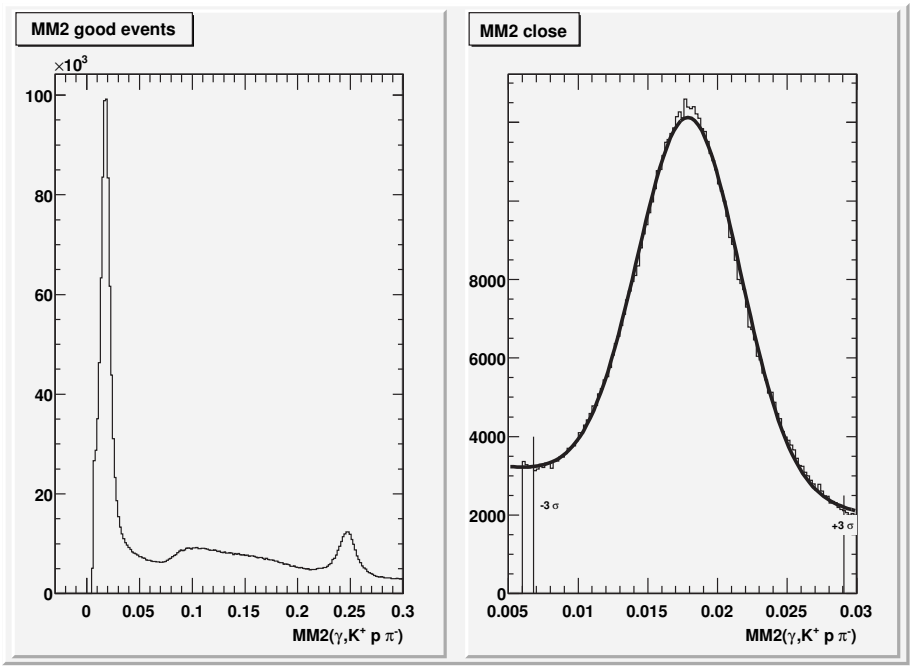

Figure 10: The entire MM2 spectrum and a close look at the missing π^0 region after the ΔTOF cuts. The entire spectrum shows the very strong π^0 peak over a background and also the peak for missing K^0 events. The fit on the right is a Guassian with a 1st order polynomial background.

For the $\Lambda(1405)$ analysis events are further chosen by various physical conditions such as the presence of a Σ^+, but we will use this sample of events as the "conventional cuts" events for the topology $p, K^+, \pi^-, (\pi^0)$. In Chapter 3 these events will be compared to those selected by the kinematic fit schemes.

3 Kinematic Fit Event Selection

To compare with the "conventional physics cuts" events, an attempt to select $p, K^+, \pi^-, (\pi^0)$ events via the kinematic fit was performed. The schemes to be compared were

1. kfit_skim : Use the kinematic fit on the kaon skim data set, no mass cut
2. kfit_comp : Use the kinematic fit on the whole compressed data set, no mass cut
3. kfit_masscut_skim : Use the kinematic fit on the kaon skim data set, mass cut used
4. kfit_masscut_comp : Use the kinematic fit on the whole compressed data set, mass cut used

Here "mass cut" refers to a very loose mass cut on the measured mass distribution of the 2 positively charged particles. The mass of each particle is calculated as $M = |\vec{P}|\sqrt{1-\beta^2}/\beta$, where $\beta = d/\text{TOF}$ is the particle's

velocity. Taking the calculated mass of the two particles as m_1 and m_2, the cut was $m_1 > 0.2$ AND $m_2 > 0.2$ AND ($m_1 < 0.9$ OR $m_2 < 0.9$) (Figs. 11, 12). There should be no overlap with the region that we are interested in and the region that was cut out. This will be shown explicitly when comparing the different kinematic fit schemes.

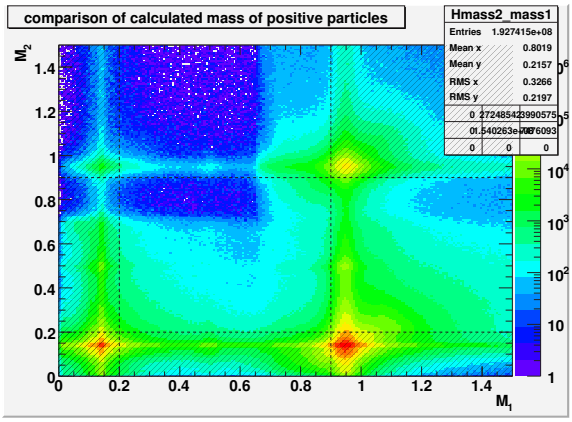

Figure 11: Mass distribution of the 2 positively charged particles' masses for the entire g11 data set. The shaded area was not used for the "mass-cut" scheme.

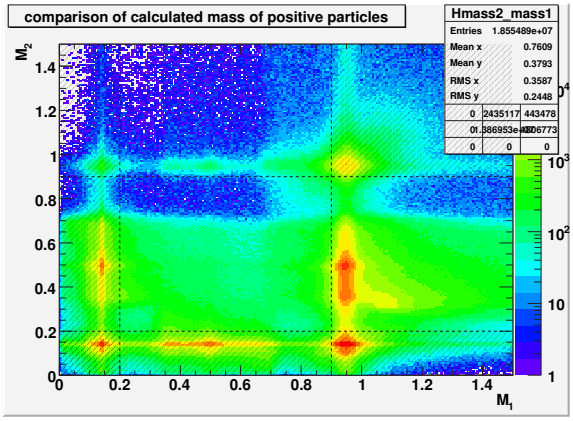

Figure 12: Mass distribution of the 2 positively charged particles' masses for the "skimmed" data set. The shaded area was not used for the "mass-cut" scheme. Notice the enhancement of (p, K^+) events compared to Fig. 11.

By using kinematic fits, events with a confidence level(CL) of over 10% for the hypothesis $p, K^+, \pi^-, (\pi^0)$ were selected. Then, to remove the background , events that had a CL of over 10% for the hypotheses p, π^+, π^- or p, π^+, π^-, π^0 were removed. For all hypotheses, an interchange of the identity of the 2 postively charged particles is possible. For the rejection cuts, all events that had a CL $> 10\%$ for either mass combination was rejected. For our selection of events, there were events that fit to both hypotheses $p, K^+, \pi^-, (\pi^0)$ and $K^+, p, \pi^-, (\pi^0)$. For these the missing mass off the kaon was computed assuming both hypotheses. This is shown in Fig. 13 and shows that the combination (p, K^+) shows the desired hyperon structure in the distribution of MM(γ, K^+) while the combination (K^+, p) does not. We therefore chose events that fit to both hypotheses to be p, K^+ combinations. This can also be inferred from the calculated mass distribution of the particles, which predominantly prefer the combination (p, K^+) over (K^+, p).

At this stage of just selecting the events with the kinematic fit, we can compare the missing mass off of the kaon as in Fig. 14. We see that there is a large excess of events in the kinematic fit schemes compared to the conventional physics cuts.

We know that we lost roughly 40% of our events due to the fiducial cuts in our conventional physics cuts, so to make the comparison meaningful, we must also apply the same fiducial cuts to the kinematic fit schemes. After applying the fiducial cuts, we arrive at Fig. 15. We now see that the kinematic fit schemes

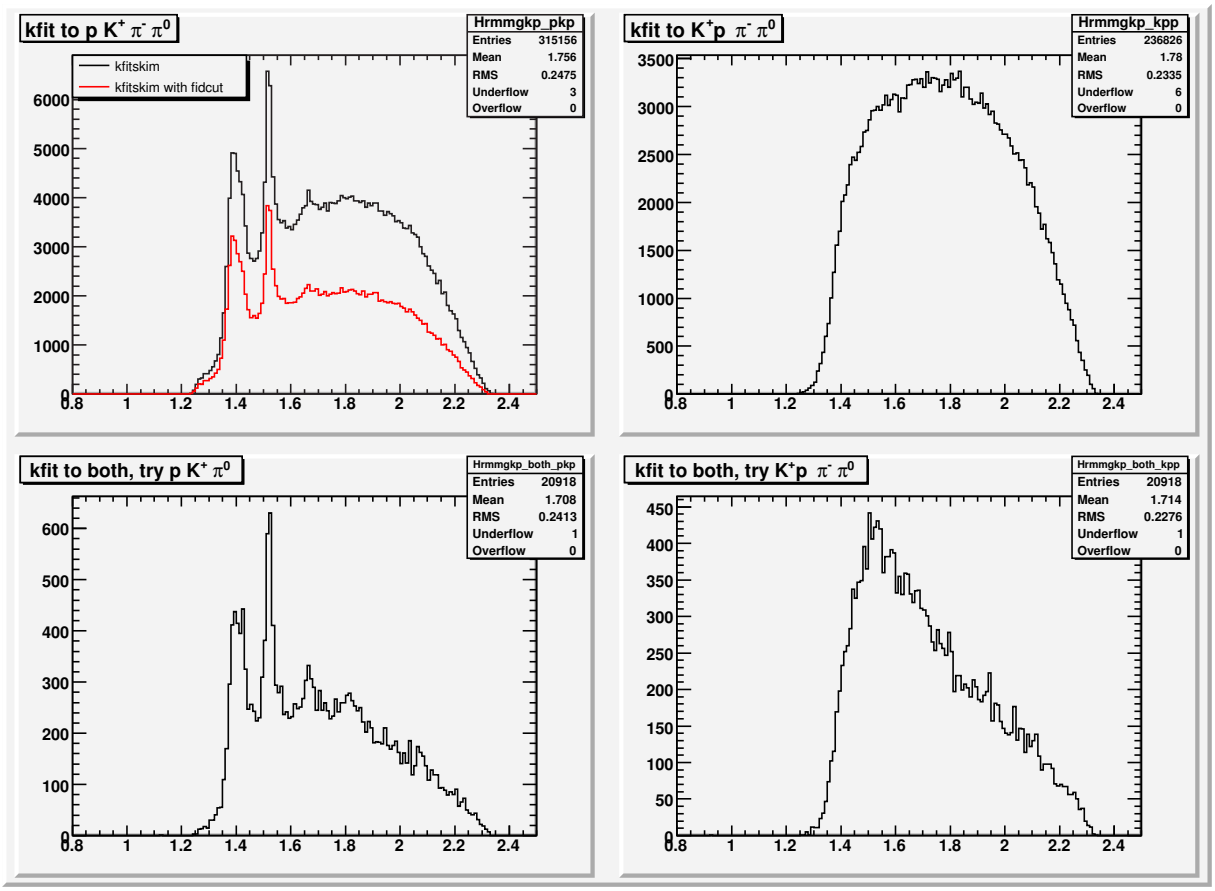

Figure 13: MM(γ, K^+) for the scheme "kfit_skim". Top row: events that fit to $p, K^+, \pi^-, (\pi^0)$ only, events that fit to $K^+, p, \pi^-, (\pi^0)$ only. Bottom row: events that fit to both hypotheses, try combination (p, K^+), and events that fit to both hypotheses, try combination (K^+, p). We see that the combination (K^+, p) does not have the desired structure.

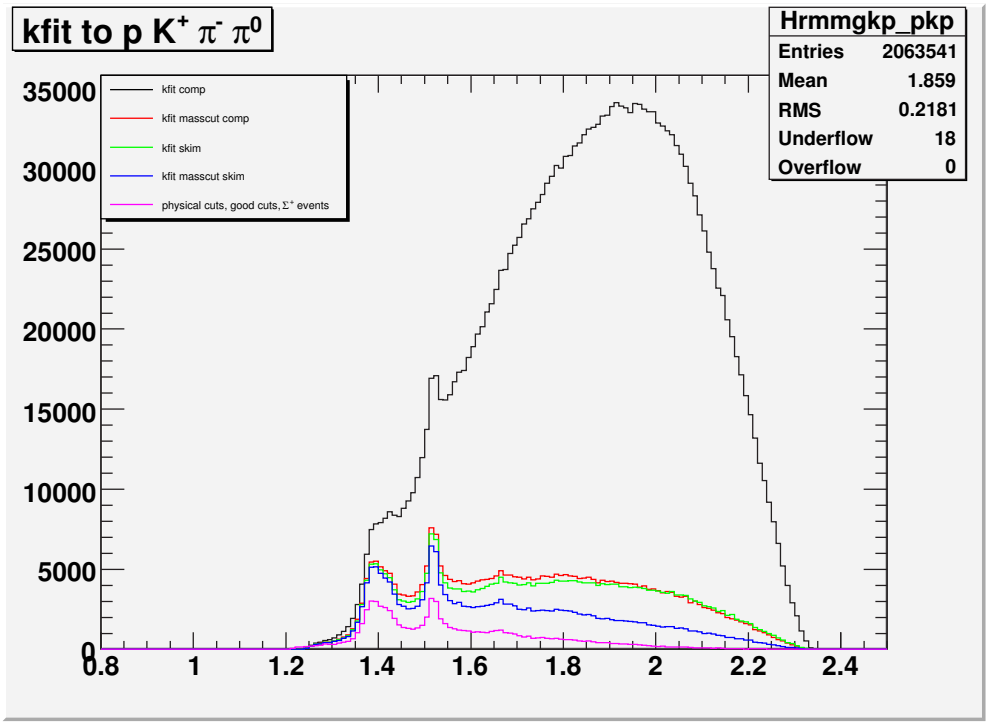

Figure 14: Comparison of MM(γ, K^+) for 5 different schemes: kfit_skim, kfit_masscut_skim, kfit_comp, kfit_masscut_comp, and conventional physics cuts.

are approaching the conventional physics cuts, but still have an excess of events, especially in the high mass region.

The events selected at this moment are events that passed the kinematic fit. But a look at the timing information of the particles shows that the timing is wrong for many of these events(Fig. 16). To get rid of these events, the same timing cut that was applied to the conventional physics cuts was alsoapplied here, resulting in the same contour as in Fig. 9. A check of the mass distribution of the two positively charged particles was done, and it was seen that for each scheme the positive particles had calculated masses close to where they should be (Fig. 17). We see that a timing cut on the particles is sufficient and there is no need to cut on the mass distribution of the positive particles.

This is the end result of the kinematic fit schemes, and we are satisfied that all four schemes coincide excellently (Fig. 18). In the next chapter we will compare these different kinematic fit schemes and the conventional physics cuts scheme. A summary of the cuts made on the kinematic fit schemes is as follows(steps in parantheses were not applied to all schemes):

1. (kaon skim)

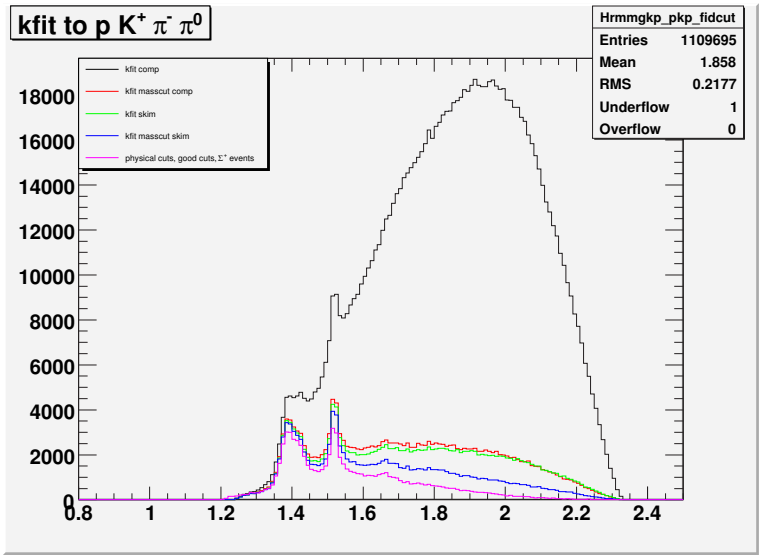

Figure 15: Comparison of MM(γ, K^+) for 5 different schemes with fiducial cuts applied: kfit_skim, kfit_masscut_skim, kfit_comp, kfit_masscut_comp, and conventional physics cuts.

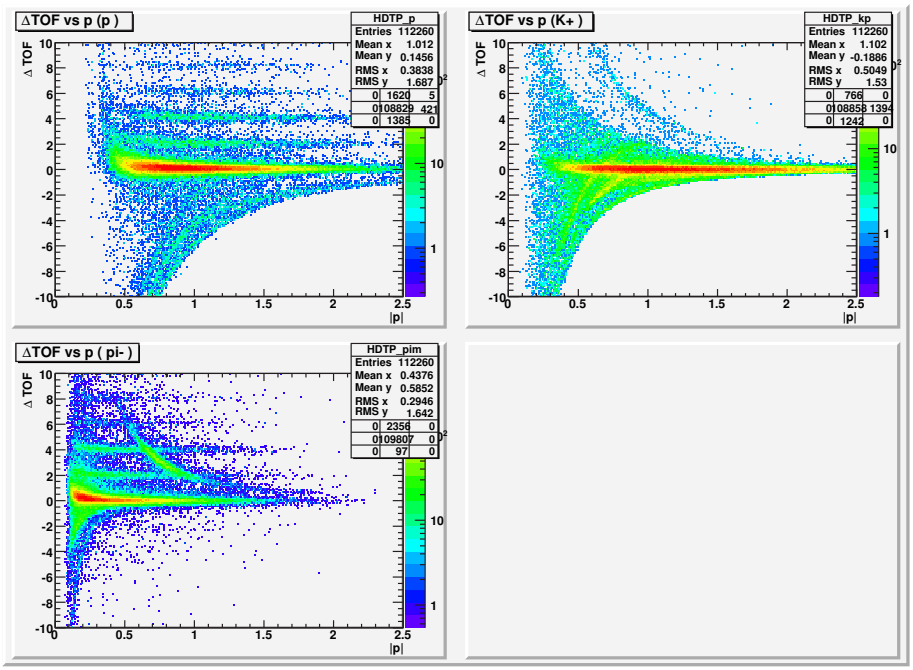

Figure 16: ΔTOF vs $|\vec{P}|$ for p, K^+, π^- respectively for the case of "kfit_masscut_skim". We see that many of the events have off-timing particles. The previously unseen band of events converging from the high side of ΔTOF to 0 for the π^-events are due to the misidentification of a K^- as a π^-.

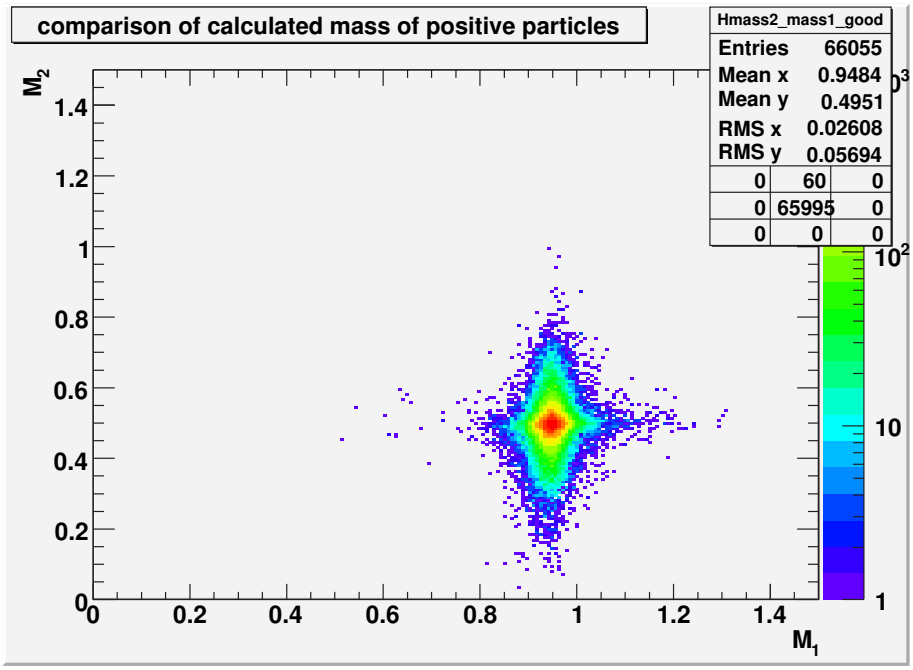

Figure 17: Calculated mass distribution of the two positively charged particles for kinematic fit events that passed the timing cut. We see that all events are distributed in the (p, K^+) region and that there is no further cut needed on the mass distribution.

2. (mass cut)
3. 10% confidence level cut on $p, K^+, \pi^-, (\pi^0)$
4. 10% confidence level rejection of p, π^+, π^- and $p, \pi^+, \pi^-, (\pi^0)$
5. ΔTOF cut

4 Comparison of the Schemes

Fig. 18 shows the final end results of our different schemes. For the distribution of missing mass off of the K^+, all four of the kinematic fit schemes coincide with each other at all but the high mass end where there are some excess events in the compressed data set. From this result we infer that at least for the topology $p, K^+, \pi^-, (\pi^0)$, which is our region of interest, there is no loss of signal due to using the skimmed data set compared to the compresed data set. Also, the loss of events compared to the conventional physics cuts can be explained by the fact that since we are using a 10% CL cut, we are losing roughly 10% of our signal.

Throughout this study the default photon timing cut of 1.5 ns was used. This is a standard cut by `part` to get rid of out of timing photons, and is on the timing difference between the photon vertex time and the "event time" calculated by `part` . To ensure that this cut was not losing any signal, all of the programs

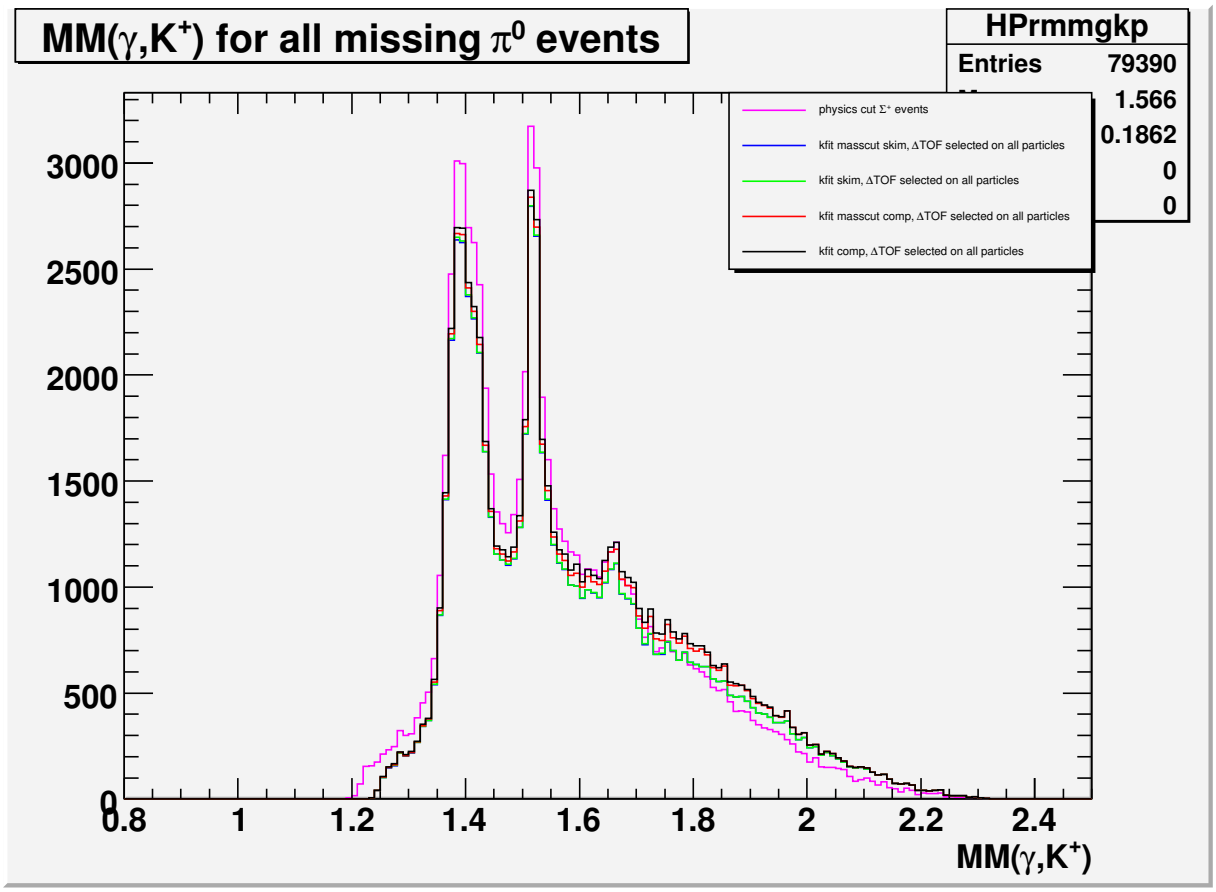

Figure 18: MM(γ, K^+) for five different schemes. Conventional cuts is for the cuts described in Chapter 2 up to the selection of a missing π^0 mass. The four kinematic fit schemes kfit_skim, kfit_masscut_skim, kfit_comp and kfit_masscut_comp. "skim" indicates that the kaon skim files were used, and "comp" implies the use of the entire compressed data set. "masscut" refers to the cut on the calculated mass distribution of the two positively charged particles in Fig. 11 The comparison is after the ΔTOF cut was made on all five schemes. The four kinematic fit schemes now agree with each other to within the % level, and have about 10% less events compared to the conventional physics cuts.

were run with the photon cut turned off. The result is Fig. 19. We see a negligible 0.02% difference in the conventional physics cuts, and for the kinematic fit schemes roughly a 2% difference for each scheme in the overall number of events that passed the cuts. We believe that this is within the other systematic errors of the experiment and do not see the need to pursue this difference further.

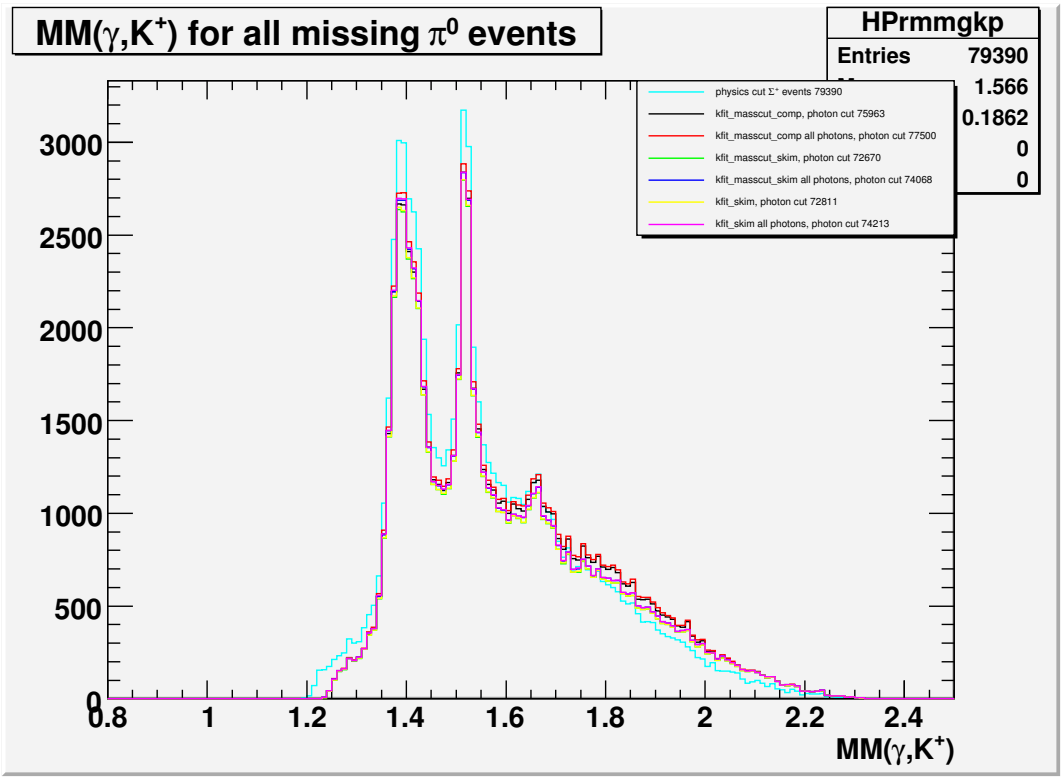

Figure 19: MM(γ, K^+) for the four different schemes physics cuts, kfit_skim, kfit_masscut_skim, kfit_masscut_comp with and without the photon timing cut. The numbers in the legend show how many events total there were for each scheme.

5 Conclusion

In this analysis note an extensive overview of the cuts made on the g11 dataset for our purpose of determining the $\Lambda(1405)$ cross section and line shape were given. For the final state topology of p, K^+, π^-, π^0, there is no obvious difference in the line shape of hyperons using the different kinematic fit schemes for event selection. We do not observe any loss of signal due to skimming of the data set. Furthermore the kinematic fit schemes agree quite well with the conventional physics cuts. These different schemes for analyzing the data will be used in future analysis for cross checks of further cuts to be made.

References

[1] M. Williams, M. Bellis, private communications